PROCEEDINGS OF THE ROYAL SOCIETY A MATHEMATICAL, PHYSICAL & ENGINEERING SCIENCES

Do dolphins benefit from nonlinear mathematics when processing their sonar returns?

T. G. Leighton, G. H. Chua and P. R. White

Proc. R. Soc. A 2012 **468**, 3517-3532 first published online 18 July 2012
doi: 10.1098/rspa.2012.0247

PROCEEDINGS OF THE ROYAL SOCIETY A

CrossMark click for updates

Proc. R. Soc. A (2012) **468**, 3517–3532
doi:10.1098/rspa.2012.0247
Published online 18 July 2012

Do dolphins benefit from nonlinear mathematics when processing their sonar returns?

By T. G. Leighton*, G. H. Chua and P. R. White

Institute of Sound and Vibration Research, University of Southampton, Highfield, Southampton SO17 1BJ, UK

Dolphins have been observed to blow bubble nets when hunting prey. Such bubble nets would confound the best man-made sonar because the strong scattering by the bubbles generates 'clutter' in the sonar image, which cannot be distinguished from the true target. The engineering specification of dolphin sonar is not superior to the best man-made sonar. A logical deduction from this is that, in blowing bubble nets, either dolphins are 'blinding' their echolocation sense when hunting or they have a facility absent in man-made sonar. Here we use nonlinear mathematical functions to process the echoes of dolphin-like pulses from targets immersed in bubble clouds. Dolphins emit sequences of clicks, and, within such a sequence, the amplitude of the clicks varies. Here such variation in amplitude between clicks is exploited to enhance sonar performance. While standard sonar processing is not able to distinguish the targets from the bubble clutter, this nonlinear processing can. Although this does not conclusively prove that dolphins do use such nonlinear processing, it demonstrates that humans can detect and classify targets in bubbly water using dolphin-like sonar pulses, raising intriguing possibilities for dolphin sonar when they make bubble nets.

Keywords: acoustics; sonar; dolphin; bubbles; clutter; radar

1. Introduction

Man-made active sonar is not accurate at identifying objects hidden in undersea bubble clouds, which attenuate and scatter the sonar beams in the manner of dense fog confounding car headlights. The scatter of the sonar 'clutters' the image in the way that backscatter from fog droplets can dominate a driver's vision, making it difficult to identify real objects of interest ('targets'). Such undersea bubble clouds are generated below breaking waves, and constitute one of the factors which can confound the use of sonar in shallow coastal waters, regions where the military have exploited the echolocation abilities of trained dolphins, for example in mine detection. Indeed, there have been rare observations of wild dolphins blowing dense bubble 'nets' to assist in catching prey (figure 1), which begs the question of whether they are 'blinding' their sonar in so doing (and therefore hunting by vision or tactile senses only) or whether they have developed a sonar that can operate in bubble clouds (Leighton 2004). Because the 'hardware'

*Author for correspondence (tgl@soton.ac.uk).

Received 21 April 2012
Accepted 20 June 2012

Figure 1. (*a*) Common dolphins herd sardines with bubble nets. (*b*) A dolphin starts to release a cloud of bubbles (arrowed) from its blowhole. A moment later (*c*) the dolphin (1) swims on, leaving behind the expanding cloud (2). Other dolphins (incl. 3) enter the frame. (*d*) The sardines school within a wall of bubbles and are trapped. Images courtesy *The Blue Planet* (BBC). (Online version in colour.)

available to the dolphin is not substantially better (in terms of power, bandwidth, etc.) than that available in man-made sonar (Au 2004; Au & Martin 2012), if they are not 'blinding' their sonar then dolphins must have some other advantage. Such an advantage might arise from, for example, the mobile platform from which they operate (their agile bodies that can insonify a target from a range of angles and perspectives), or in their auditory systems and brains, which have evolved using echolocation in bubbly water over millions of years.

This paper asks whether there is a way by which dolphins might process their signals to distinguish between targets and clutter in bubbly water. The object is not to show that dolphins use such a method, but to negate the possibility that no such option exists for solving this mystery. The authors previously proposed a form of sonar signal (TWIPS: twin inverted pulse sonar) that could work in bubble clouds, consisting of pairs of pulses that were identical except that one was inverted with respect to the other, that could detect targets in bubbly water if the signal processing were to make use of nonlinear mathematics (Leighton 2004). TWIPS worked in simulation, tanks tests and finally sea trials, detecting targets in the wakes of a ferry and a commercial ship of 3953 and 4580 gross register tonnage, respectively (Leighton *et al.* 2010, 2011). However, while these TWIPS

pulses were successful, there is no conclusive evidence that the types of pulses devised for that study are used by any type of dolphin (Leighton *et al.* 2010; Finfer *et al.* 2012). In this paper, a more general form of nonlinear mathematical processing is applied to pulses based on models of dolphin echolocation clicks. This biased pulse summation sonar (BiaPSS) reduces the effect of clutter by relying on the variation in click amplitude (such as that which occurs when a dolphin emits a sequence of clicks), rather than relying on the formation of inverted pulses that are used by TWIPS. BiaPSS is shown by tank experiments to be effective in distinguishing targets from the clutter generated by bubbles in the 'field of view' of the sonar. While this does not prove that dolphins are capable of undertaking such nonlinear mathematical processing, it establishes the fact that such processing makes these dolphin pulses effective in bubbly water for distinguishing between targets and clutter, which is not achieved by the standard sonar processing used here on the same data.

Section 2 outlines the method. The results in §3 explore three cases. The first case reports on BiaPSS processing test tank data for an experimental pulse that is as close as the available equipment can generate to a waveform that is commonly accepted to typify a form of emission from the Atlantic bottlenose dolphin (*Tursiops truncatus*). The second case undertakes a similar study for a linear frequency-modulated (LFM) pulse. Both of these tank test cases are used to validate a simulation scheme described by Chua *et al.* (2012). Having conducted such a validation, this simulation is applied to test the efficacy of BiaPSS processing on the typified Atlantic bottlenose dolphin emission, which we are not able to create in the test tank with the available transducers.

2. Method

The Atlantic bottlenose dolphin is typical of dolphin species in that, when echolocating for a target, they emit a sequence of consecutive clicks. There are numerous echolocation studies on the Atlantic bottlenose dolphin that indicate that such signals are of short duration (50–80 µs), high intensity (up to 228 dB re 1 µPa peak-to-peak at 1 m range) and broadband (Au 1993; Au & Nachtigall 1997). Each click can be modelled as two synchronous chirps, each covering a distinct frequency range and both being down-chirps (i.e. decreasing in frequency as time progresses; Capus *et al.* 2007). These clicks will be reflected back from scattering objects in the water, some of which might be targets of interest (e.g. prey) and some of which will be 'clutter' (strong scatterers that are not targets of interest but that might be confused as such by the dolphin when it interprets the sonar).

The pulse used in the experiments of §3*a* contains most of its energy at frequencies between 50 and 110 kHz, which are within the typical range found in dolphins' clicks. However, to reduce demand and to keep within the capabilities of the transducer, the pulse used in this experiment (figure 2) has a lower amplitude (making this a conservative test from that perspective because lower amplitudes excite weaker nonlinearities from the bubbles), and has a duration of 120 µs (figure 2), longer than the 50–80 µs typical for dolphins. This is therefore not an actual dolphin pulse, but as representative a test as the hardware can deliver within the model outlined by Capus *et al.* (2007). Section 3*b* uses LFM pulses

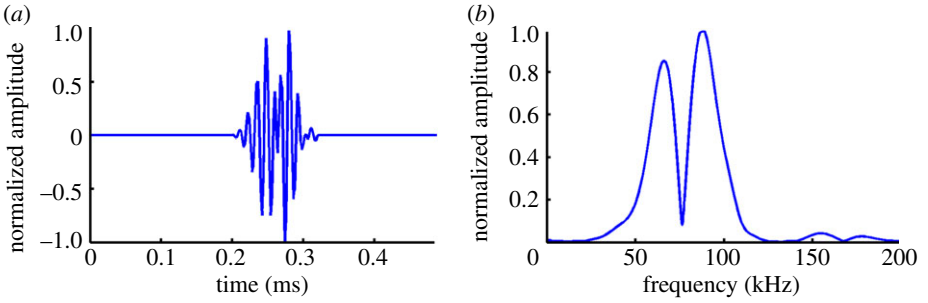

Figure 2. The pulse used in the tank experiment presented in (*a*) time domain and (*b*) frequency domain with a peak-to-peak amplitude of approximately 220 dB re 1 µPa m. (Online version in colour.)

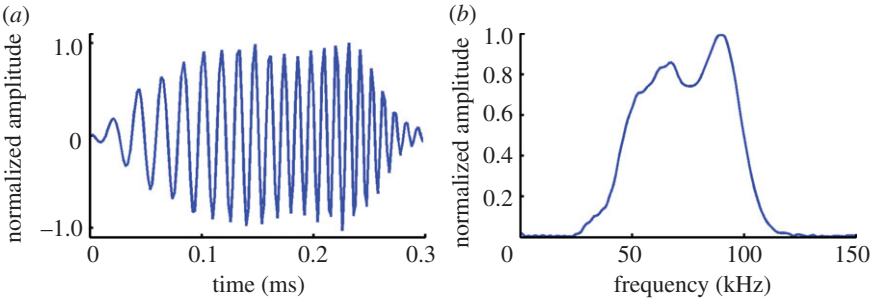

Figure 3. The LFM pulse used in the sonar simulation model and tank tests measured at 1 m from the source. The LFM pulse varied from 30 to 110 kHz over a duration of 300 µs. The amplitude of the first pulse shown in (*a*) was approximately 15% of that of the second pulse (not shown). The second pulse has a peak-to-peak amplitude of approximately 218 dB re 1 µPa m. The frequency domain representation of the first LFM pulse is shown in (*b*). (Online version in colour.)

(which are not used by dolphins for echolocation; figure 3), and §3*c* reports simulation results of the dolphin-like pulse described by Capus *et al.* (2007) (figure 4).

Bubbles are a particularly potent form of clutter for echolocation. This is demonstrated by generating a bubble cloud in a freshwater tank measuring $8 \times 8 \times 5$ m at the Institute of Sound and Vibration Research, University of Southampton, UK. The bubbles in the cloud have a size distribution and density resembling that found in the ocean (see Leighton *et al.* (2010) for details). The sonar source is placed in the water tank with a target (of target strength of −38 dB) placed at a distance of 0.8 m from the source, as shown in figure 5. The target is a 0.05 m diameter solid steel sphere. The sonar source used is a custom-made transducer, supplied by Neptune Sonar Ltd. This source operates within a frequency bandwidth between 30 and 120 kHz, powered by a wideband amplifier designed to improve the fidelity of the waveform generated (Doust & Dix 2001). The source's beamwidth has been measured in the 40–100 kHz range, where the 3 dB beamwidth is reported as 10° to 30°. A single omnidirectional hydrophone is used (Blacknor Technology, D140 with built-in preamplifier, calibrated by the National Physical Laboratory) with a flat frequency response

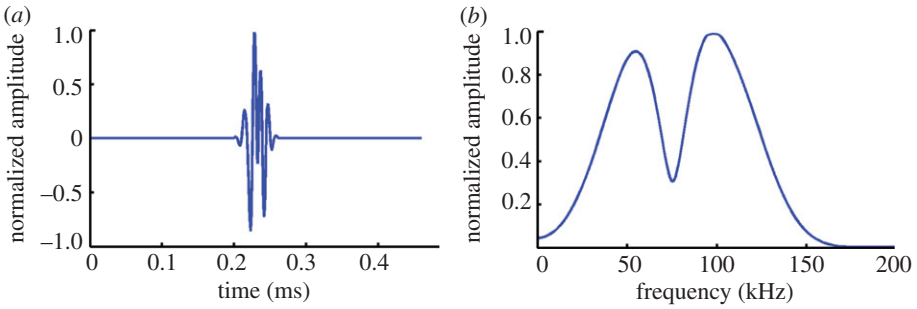

Figure 4. The 'dolphin' pulse used in the simulation presented in (*a*) time domain and (*b*) frequency domain with a peak-to-peak amplitude of approximately 226 dB re 1 µPa m. (Online version in colour.)

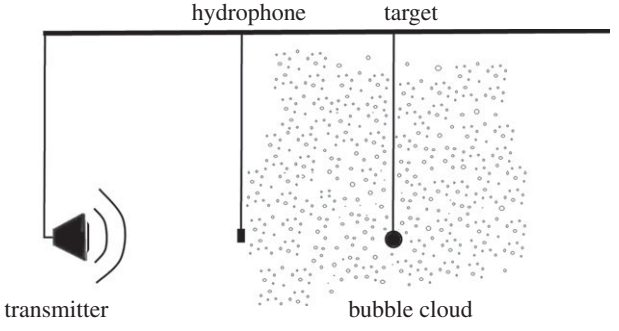

Figure 5. The set-up in the tank test (not to scale).

(±3 dB) up to 150 kHz. A train of pulses is emitted, such that the interval between each pulse pair is 0.5 s. The separation between the pulses in each pulse pair is kept at 15 ms. Although this is of similar order to the minimum inter-click time quoted by Au (1993), here 15 ms is not set for biological reasons but instead simply chosen to exceed the reverberation time of the tank at these frequencies (10 ms). It is well within the maximum allowable inter-click time in this tank, set because BiaPSS processing, like TWIPS processing, assumes that the field of scatterers (here particularly the bubble cloud) does not evolve significantly during the interval between the start time of the two pulses (Leighton *et al.* 2010). The exact value for this upper limit thus depends strongly on prevailing environmental conditions. For the tank tests carried out, one critical factor will be the motion of the bubbles through buoyancy in the tank (there is little turbulence in the test environment and the sensor system is rigidly mounted). To obtain an estimate of this upper limit, the insonified width can be compared with the motion of the bubbles in the two-dimensional case. Using a sonar beamwidth of 10°, this translates to an insonified width of approximately 0.18 m at a distance of 1 m. Using a rising speed of 30 cm s^{-1} (this being the upper bound speed for the range of bubble sizes present in the tank bubble population (Clift *et al.* 1978)), a conservative estimate of 60 ms is obtained for a 10 per cent change in the insonified cloud. The 15 ms chosen is well within this maximum value.

In a given click train in the experiment of §3*a*, every alternate pulse is as shown in figure 2*a*, but between them are pulses that have the same form as that of figure 2*a* but with the amplitudes all scaled down to approximately 30 per cent. This is done to investigate whether this change can be exploited using a proposed detection algorithm BiaPSS. The algorithm is tested with the pulses of figures 2–4 specifically to test (i) whether BiaPSS is effective at classification, i.e. at distinguishing between genuine targets and clutter, and (ii) whether BiaPSS improves target detection, which is tested using the standard method of producing receiver operating characteristic (ROC) curves. Note that a ROC curve only gives a measure of the detection performance and not the ability to provide classification. Leighton *et al.* (2010, 2011) found that TWIPS was very effective at task (i), and could generate some improvements at task (ii).

If BiaPSS were found to be effective, particularly with the dolphin-like pulses characterized by Capus *et al.* (2007), then it raises the unanswered question of whether an algorithm similar to BiaPSS is exploited by dolphins, such that the observed change in amplitude of pulses in a dolphin click train is important to clutter reduction and classification in their sonar. Given that the algorithm requires use of nonlinear mathematics, this possibility might seem remote, but the efficacy of BiaPSS processing with dolphin-like pulses would make it an intriguing question.

It has indeed been observed that the amplitude of the clicks emitted by a dolphin can change during a single click sequence (Au & Nachtigall 1997; Herzing & dos Santos 2004; Houser *et al.* 2005). Consider the following thought experiment. If two successive clicks are emitted, and the second pulse is identical to the first in every way except that its amplitude is one-third that of the original pulse, then provided that all aspects of the environment (ocean, target and clutter) stayed the same, one might expect the echoes from the target to be identical except that the second echo has one-third of the amplitude of the first echo. If the dolphin were mentally to triple the amplitude of the echo from the second click, and subtract it from the first click, the result would be zero. If the dolphin knows the factor by which the amplitude of the clicks changed when it emitted them, it could use that factor in the corresponding processing of the echoes, in place of the factor of 3 used in the thought experiment. While this would work for a linearly scattering target, this would not work for all the energy scattered by bubbles. This is because, when driven with a sound field of sufficient amplitude, the bubbles scatter nonlinearly (for example, as the square of the amplitude of the incident pulse). As a result, changes in the amplitude of the pressures that drive the bubbles do not match the scale factors seen in the signal scattered back by the bubbles. In the earlier mentioned thought experiment, the echoes from the bubbles of the first pulse are not three times those of the second pulse from the same bubbles. The subtraction of the scaled echoes from the two pulses of different amplitudes described earlier does not result in zero for a nonlinear scatterer like a bubble. Subtraction of the scaled echoes (from the two pulses) does not make the echoes from the bubbles disappear from the image, as it does for the target. In this way, images can be formed that show the position of the clutter (bubbles), and that do not show the target. Similarly, weighted addition of the two echoes can enhance the linear scattering from the target and partially suppress the bubble clutter, as detailed later.

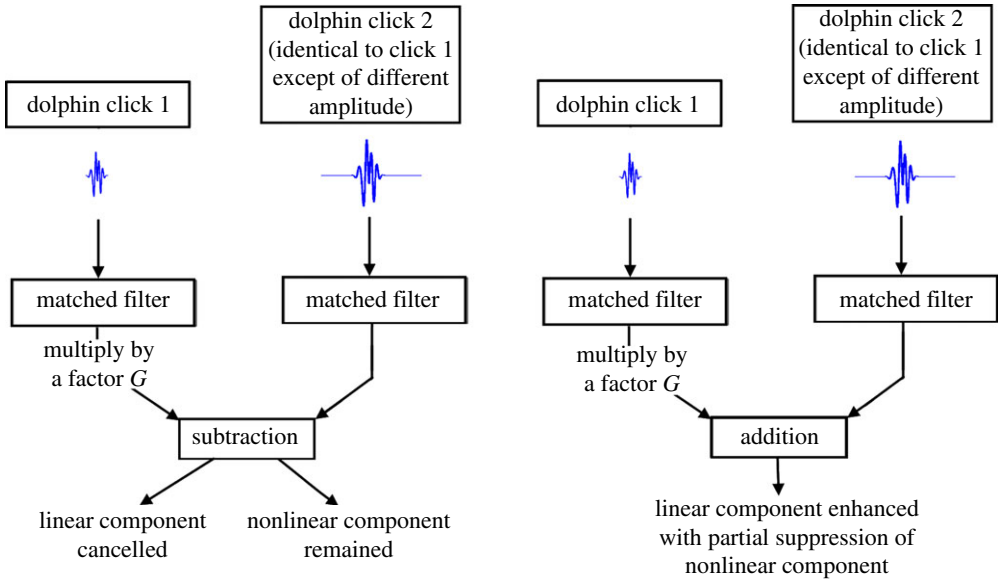

Figure 6. Processing scheme by which the echoes from a pair of dolphin-like pulses of different amplitude are processed to enhance/cancel the nonlinear/linear components of the scattering through weighted subtraction and addition of the scattering. The magnitude of the second pulse is greater than that of the first pulse by a factor of G. (Online version in colour.)

This processing scheme can be described in simplified form through the scattering of two adjacent pulses in a click train (figure 6). Consider that, within a train of $2N$ pulses, a pulse, $c_1(t)$, of duration T is followed, after an interval of τ, by a similar pulse, $c_2(t)$, of different amplitude. These pulse pairs are emitted with a period of Δ. If this pair sequence is repeated (BiaPSS does not require this to be the case), the resulting pulse train can be expressed as $p(t) = \sum_{n=0}^{N-1} c_1(t - n\Delta) + c_2(t - \tau - n\Delta)$. Assuming a linear model of propagation and scattering, including a linearly scattering target (which can be taken here to represent a fish excited at much higher frequencies than the resonance of its swim bladder), the signal at the receiver, $y(t)$, can be modelled as the convolution of this signal with an impulse response, $h(t)$. This impulse response models the two-way propagation from source to target and the target's scattering characteristics. Accordingly, the model for the received signal is $y(t) = \sum_{n=0}^{N-1} y_1(t - n\Delta) + y_2(t - \tau - n\Delta)$ in which $y_k(t)$ (where $k = 1, 2$) represents the convolution of the incident pulse and the impulse response function, specifically $y_k(t) = h(t) * c_k(t) = \int h(t - t')c_k(t')\,dt'$. If $c_2(t)$ is greater than $c_1(t)$ by a factor of G, and used as the new excitation, the response $y_2(t)$ is then given by $y_2(t) = h(t) * c_2(t) = Gy_1(t)$. Assume that the detection system uses a matched filter (Burdic 1984) that is scaled such that its overall gain is unity. In such circumstances, if the outputs of the matched filter for $y_k(t)$ are denoted $Y_k(t)$ (where $k = 1, 2$), it follows that $Y_2(t) = GY_1(t)$. Therefore, the subtraction of $GY_1(t)$ from $Y_2(t)$, which will be termed P_- in this paper, is zero for a linear scatterer. This applies not just to the steady-state linear scatter but also to linear scatter associated with ring-up (Clarke & Leighton 2000) and ring-down (Leighton *et al.* 2004). This allows BiaPSS to discriminate between such linear targets and nonlinear scatterers like bubbles,

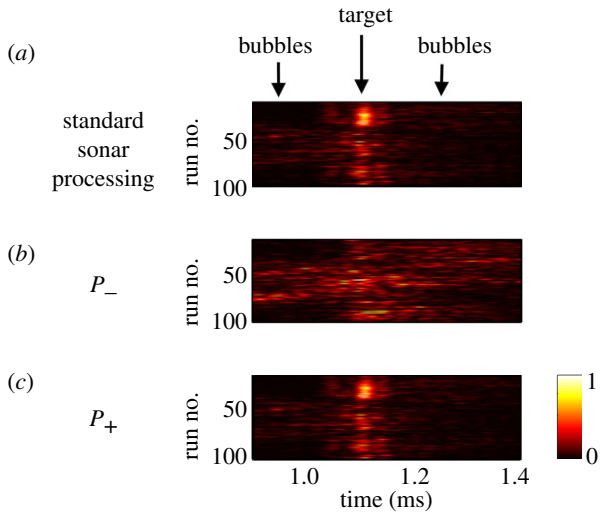

Figure 7. Normalized plots of tank experiments using the dolphin-like pulse pair of §3*a* where (*a*) is the standard sonar processing, (*b*) P_- and (c) P_+ processing of the two return signals with one appropriately scaled. The plot is normalized to the maximum value within each plot. The values are 2.2×10^2, 5.5×10 and 1.7×10^3 for (*a*), (*b*) and (*c*), respectively. Arrows above each panel indicate the position where the target should appear, and some of the bubble locations (which are present throughout the frame). (Online version in colour.)

which will in general have a non-zero value for P_-. This is because, for a nonlinear system, the scattering from a pulse of different amplitude does not scale with the linear gain G. The addition of $Y_2(t)$ and $GY_1(t)$, referred to as P_+ in this paper, tends to enhance the linear components of the scattered signal relative to the nonlinear ones. Such processing will not lead to the complete removal of nonlinear components, but only serve to suppress them partially. This approach can be regarded as a generalization of the TWIPS principle (Leighton *et al.* 2010, 2011), with TWIPS corresponding to the choice of $G = -1$, albeit that, in that instance, the roles of P_+ and P_- are reversed. The website where the data can be obtained is listed in the acknowledgements.

3. Results

(*a*) *Results for dolphin-like pulses*

Figure 7*a* stacks side-by-side the received echoes from pairs of pulses to form an 'echogram' image. In each pair, the second pulse is approximately 30 per cent the amplitude of the first pulse, as described in §2. In figure 7*a*, the pairs of pulses are processed using 'standard sonar processing' (which for each plot shows the average energy of the two clicks with that energy being calculated by first matched-filtering the return signals, and then temporally averaging the envelope of the resulting signal over a time based on the spatial resolution of the matched filter). In figure 7*a*, the target cannot be distinguished from the bubble clutter (both labelled), which would enable prey to hide from the echolocation of a dolphin, and mean that during bubble netting, or under breaking waves, a dolphin would have to rely on vision only to hunt.

Figure 7*b* uses exactly the same set of raw echo data as figure 7*a* but processes them in the BiaPSS manner described in §2 to ensure that, whatever is a real target, disappears from the image, leaving only the bubbles. To be specific, the subtraction of the return signals from the two pulses, with the smaller waveform of the pair scaled up by $1/0.3 \approx 3.3$, is matched-filtered, and then temporally averaged. This is denoted by P_-. The computed values of P_- are then similarly stacked side-by-side over 100 runs and presented in figure 7*b*. The environment is not completely static as in the thought experiment, as the bubble cloud moved between the two pulses, but the level of degradation this causes in the cancellation of the target scatter is not sufficient to impair the result significantly.

In similar vein, if the echo from the second pulse were to be multiplied by 3 (or by whatever factor the dolphin from the thought experiment used in reducing the amplitude of the second click with respect to the first), then when the echoes of the consecutive pulses were added to one another, the backscatter from the linear target would remain in the image. Figure 7*c* shows the normalized plot with the addition of the returned signals from the two pulses after multiplication by the appropriate gain constant, 3.3 (denoted as P_+). For consistency, matched-filter processing and temporal averaging have been implemented in figure 7*c* as in all plots in figure 7. However, it is noted that the backscatters from the target can be similarly distinguished from the bubble clutter by simple subtraction and addition of appropriately scaled return signals without using matched-filter processing. In this way, a dolphin could (if it could perform subtraction and addition) distinguish the target (which remains in figure 7*a*,*c* but is suppressed in figure 7*b*) from the bubble clutter (which is enhanced in figure 7*b*). This can be done for the same set of received echoes, as there is no need to send out different pulses for the two processes. A human operator could readily identify the target by visually alternating between the P_- and P_+ images, the target being the object that flashes 'on' in P_+. This ability to distinguish between a target and clutter would remove the confusion inherent in standard sonar processing of exactly the same data (as shown in figure 7*a*).

The earlier mentioned example illustrates the ability of BiaPSS to discriminate between targets and bubble clutter. As with TWIPS (Leighton *et al.* 2010, 2011), such effectiveness at discrimination is seen as its primary advantage, an enhancement of the ability to detect the target in the first place (prior to classifying it) being a secondary, lesser advantage. Figure 8 compares the ROC curve for BiaPSS processing of this dolphin-like pulse for tank data (figure 8*a*) and for simulation (figure 8*b*) (using the simulation method described by Chua *et al.* (2012)). In the simulation, the losses during transmission to and from the bubble cloud are imposed by applying the attenuation that would be given by linear bubble pulsations (Commander & Prosperetti 1989), the attenuation of water (Francois & Garrison 1982*a*,*b*) and geometric losses. ROC curves reflect the ability of a sensor to detect a target, though they are blind to the abilities in classification described earlier. ROC curves plot the probability of a true positive (P_d) on the vertical axis against the probability of a false alarm (P_fa) on the horizontal axis. The most useless sonar system follows the 45° line (shown in the figures) as this equates to 'flipping a coin' to decide whether a sonar contact is a genuine target or clutter. The difference between the ROC curves for the experiment and simulation in figure 8 is explained by the fact that the model fails to reproduce certain aspects of the specific bubble cloud in the tank. In particular, the cloud

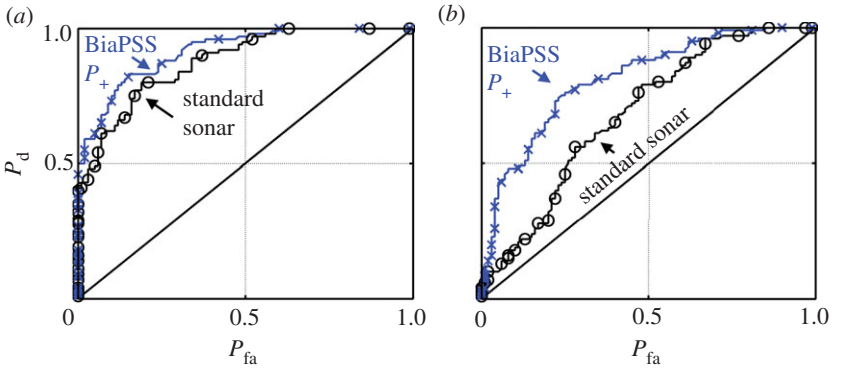

Figure 8. ROC curves for the dolphin-like pulse pair of §3*a*, computed from (*a*) tank data and (*b*) simulated data. Both curves show the result for P_+ (cross symbols) and standard sonar processing (circles). (Online version in colour.)

formed in an experiment will exhibit spatial and temporal heterogeneity that the model is unable to replicate precisely. The absolute performance, as measured by the ROC curves, of the model relative to the experiment suggests that this environmental feature is not perfectly modelled. Both of the ROC curves in figure 8 show improved performance for BiaPSS over standard sonar processing, as the BiaPSS curve is consistently above the standard sonar, meaning that, for every detection, it produces fewer false alarms. False alarms can be damaging to missions. They could cause a dolphin to be distracted from a genuine fish by bubbles and waste valuable energy chasing bubbles during a hunt. If false alarms occur in man-made sonar, they can needlessly delay a vessel's progress by causing it to reduce speed and deploy mine-hunting divers, change mission plan, etc.

(*b*) *Linear frequency-modulated pulses*

Similar tests were undertaken using LFM pulses of 300 µs duration (figure 3). Here, a solid sphere (of target strength of −30 dB) is placed at a distance of 0.85 m, in a set-up as shown in figure 5. The solid sphere is made of steel and is 0.12 m in diameter. Tank measurements of the ability of BiaPSS to distinguish a linear target from bubble clutter (figure 9) resemble simulation of the same situation made using the method of Chua *et al.* (2012) (figure 10). As with the dolphin-like pulse of §3*a*, BiaPSS works with LFM pulses to provide effective classification between the linear target and the bubble clutter. This is because the target must be the feature, which is strong in figures 9*c*(i) and 10*c* but invisible in figures 9*b*(i) and 10*b*. BiaPSS is also able to enhance detection ability with LFM pulses, as indicated by the ROC curves of figure 11.

(*c*) *Simulation of BiaPSS for 'dolphin' signals*

Although the apparatus described in §2 was not sufficient to generate what would be considered 'dolphin' pulses in the tank, these can be tested in simulation using the methods from the preceding sections. Figure 4 shows the 'dolphin' pulse used in the simulation. This 'dolphin' pulse is based on the model of

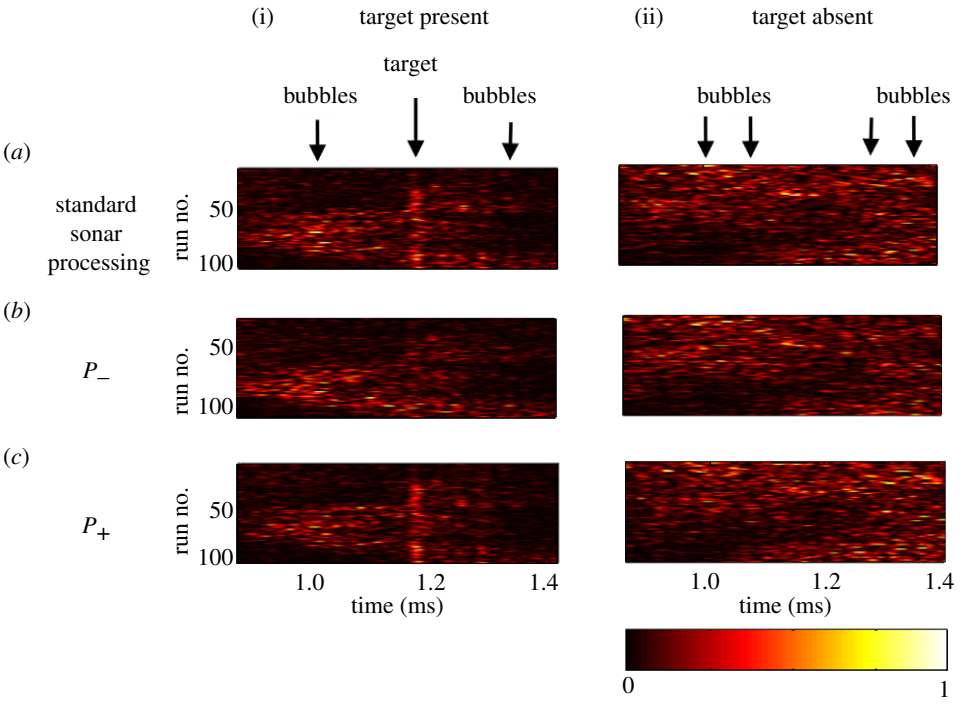

Figure 9. Normalized plots of tank experiments using the LFM pulse pairs where (*a*) is the standard sonar processing, (*b*) P_- and (*c*) P_+ processing of the two return signals with one appropriately scaled. The plot is normalized to the maximum value within each plot. The values are 6.5×10, 2.3×10^2 and 4.2×10^2 for (i)(*a*), (i)(*b*) and (i)(*c*), respectively, for the target present case. For the target absent case, the values are 3.8×10, 1.7×10^2 and 1.7×10^2 for (ii)(*a*), (ii)(*b*) and (ii)(*c*), respectively. Arrows above each panel indicate the position where the target should appear, and some of the bubble locations (which are present throughout the frame). (Online version in colour.)

Capus *et al.* (2007), which can be taken to be an appropriate representation of a real dolphin pulse for engineering purposes. The 'dolphin' pulse used there has a similar waveform. Figure 12 shows the simulated results for its performance if it were to be deployed in a bubble-filled environment. The bubble-filled environment is represented by a uniformly distributed bubble population, with size distribution being similar to that in the tests of §§2 and 3*a*,*b*. Here, the linear target will be represented by a linear scatterer with a target strength of −41 dB placed at a distance of 1.25 m from the 'dolphin'. This value of −41 dB is chosen as it is within the typical range of target strength of some fish species, with fish length of approximately 15–30 cm (Au *et al.* 2007). For this target and bubble population, standard sonar processing detects both target and bubbles (a much weaker target would not be detectable, of course). But standard sonar does not provide a way of proving which is which (the visual cues to the human of the straight line in figure 12*a* would not be present when hunting a moving fish). As before, BiaPSS is clearly able to identify the target by its appearance in figure 12*c* and disappearance in figure 12*b*. In addition to this effectiveness at distinguishing between a linear target and bubble clutter, BiaPSS also provides enhanced target detection with this 'dolphin' pulse pair, as shown by the ROC curve of figure 13.

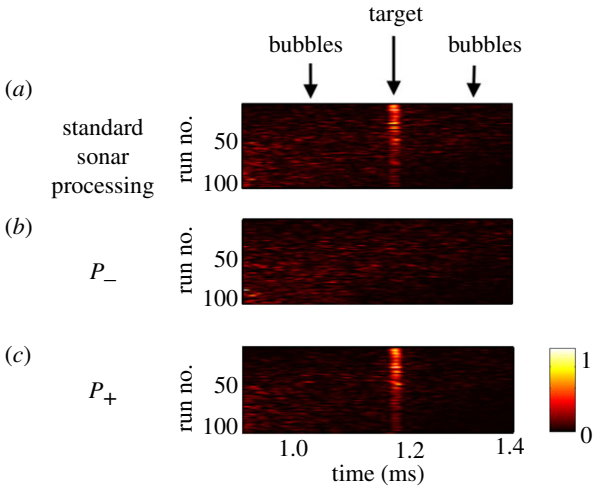

Figure 10. Normalized plots of simulations using the LFM pulse pair of §3*b* where (*a*) is the standard sonar processing, (*b*) P_- and (*c*) P_+ processing of the two return signals with one appropriately scaled. The plot is normalized to the maximum value within each plot. The values are 5.8×10^{10}, 1.3×10^{11} and 4.1×10^{11} for (*a*), (*b*) and (*c*), respectively. Arrows above each panel indicate the position where the target should appear, and some of the bubble locations (which are present throughout the frame). (Online version in colour.)

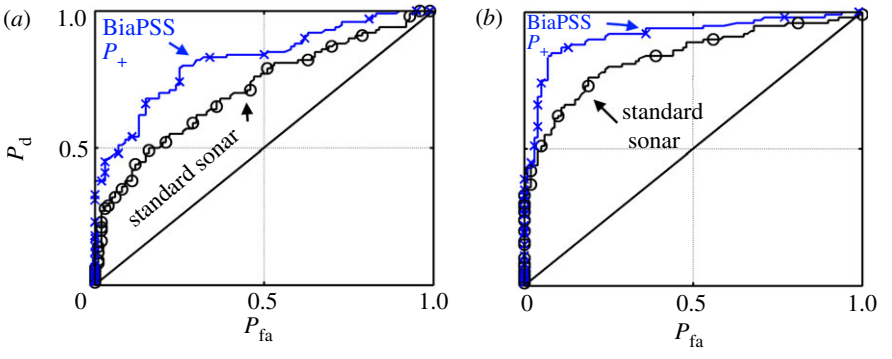

Figure 11. ROC curves for the LFM pulse pair of §3*b*, computed from (*a*) tank data and (*b*) simulated data. Both curves show the result for P_+ (cross symbols) and standard sonar processing (circles). (Online version in colour.)

It would be misleading to extrapolate these data to make general comparisons between pulse types. Here, BiaPSS processing appears to work best with the LFM pulse when compared with standard sonar processing: in tanks tests, the probability of a true positive (before giving a single false alarm) improves from 7 to 38 per cent and the area under the ROC curve increases by 16 per cent (figure 11*a*). In contrast, for tank data with the dolphin-like pulse (figure 8*a*), the probability of a true positive (before giving a single false alarm) improves only from 41 to 50 per cent, and the area under the ROC curve increases

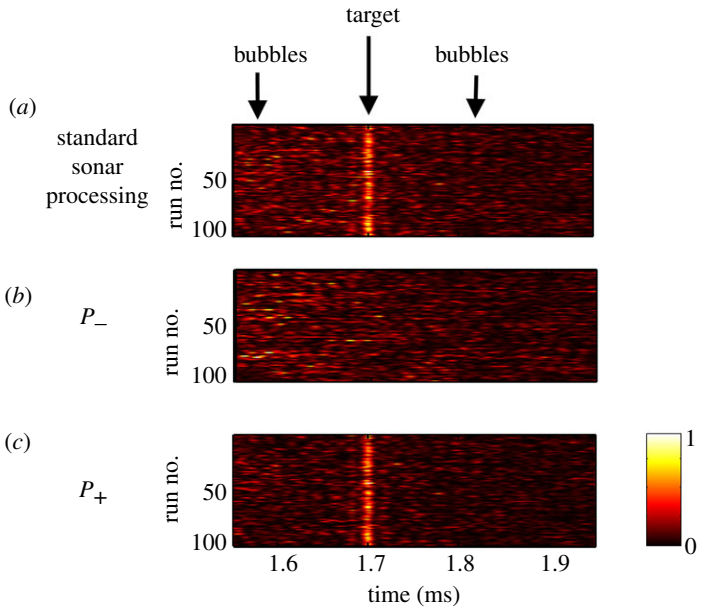

Figure 12. Normalized plots of simulations using a 'dolphin' pulse pair of §3*c* where (*a*) is the standard sonar processing, (*b*) P_- and (*c*) P_+ processing of the two return signals with one appropriately scaled. The plot is normalized to the maximum value within each plot. The values are 1.3×10^9, 3.1×10^9 and 7.8×10^9 for (*a*), (*b*) and (c), respectively. Arrows above each panel indicate the position where the target should appear, and some of the bubble locations (which are present throughout the frame). (Online version in colour.)

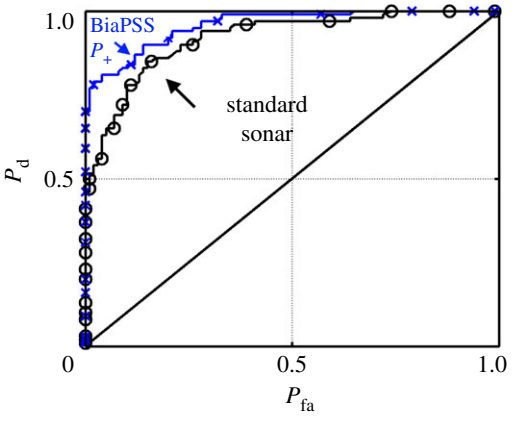

Figure 13. ROC curves for the 'dolphin' pulse pair of §3*c*, computed from (*a*) tank data and (*b*) simulated data. Both curves show the result for P_+ (cross symbols) and standard sonar processing (circles). (Online version in colour.)

only by 4 per cent with BiaPSS against standard sonar. For the 'dolphin' signal simulations (figure 13), the probability of a true positive (before giving a single false alarm) improves from 46 to 70 per cent and the area under the ROC curve increases by 4 per cent with BiaPSS when compared with

standard sonar. However, these comparisons follow from the fact that BiaPSS works better the greater the degree of nonlinearity that can be excited from the bubbles. The available source was limited to a maximum amplitude, and the tank data were taken with pulses generated at that amplitude. Although both the dolphin-like pulses (figure 8*a*) and the LFM pulses (figure 11*a*) therefore had the same maximum amplitudes, the shape of the LFM waveform meant that it contained greater energy, and therefore excited a greater degree of nonlinearity, and therefore performed better in these particular tests.

4. Conclusions

BiaPSS has been shown to be effective at distinguishing between bubbles and linear targets in tank tests and simulations using: emissions as close to dolphin-like sonar pulses as the available equipment would allow (§3*a*); and LFM pulses (§3*b*). Having validated the simulation method with such related cases, the simulation is used to show the efficacy of BiaPSS with the dolphin-like pulses characterized by Capus *et al.* (2007). This paper has provided no evidence that dolphins do use nonlinear mathematics in processing sonar returns. However, it proves that there is a workable solution to the enigmatic question of why dolphins would hunt with bubble nets if, by doing so, they 'blind' their spectacular sonar system.

Questions remain, which would require data from dolphins to address. For BiaPSS to work efficiently, the receiver would be expected to have an upper frequency limit of at least twice the centre frequency of the pulse used. The audiogram of the Atlantic bottlenose dolphin is reported to have an upper frequency limit of 150 kHz, and the majority of their echolocation clicks have a peak frequency that lies between 110 and 130 kHz (Au 1993). Such figures suggest that dolphins cannot access the majority of the information in the signals necessary to exploit such strategies. It should be noted that dolphins adapt their echolocation pulses to suit their environment (Houser *et al.* 2005). To exploit nonlinear processing, such as BiaPSS, dolphins would be expected to use pulses with lower peak frequencies, below 75 kHz, a value that is well within the range observed in the absence of bubble production (Au 1993; Houser *et al.* 2005). If future tests were not to show dolphins adjusting their clicks to transmit significant energy below half of their upper frequency hearing limit when echolocating in bubbly water, the possibility that they are using nonlinearities in the way described in this paper would be remote.

As with many hunts, rapid movements in the target (the fish) and the environment (the bubble cloud) can assist the prey in evading capture, and only bubble motion was included (in both experiments and simulations) here.

The reason for the observed variation in click amplitude produced by dolphins has never been fully explained. BiaPSS favours large changes in amplitude between adjacent pulses and a statistical examination of amplitudes in dolphin click trains would be an obvious next step.

As with TWIPS, BiaPSS has a range of applications for man-made technologies, for example in detecting targets, particularly if they can be made to scatter nonlinearly. While nonlinear scatter can be obtained from the swim bladders of fish, it occurs when they are driven at much lower frequencies

than those used by echolocating dolphins. Consequently, fish would represent substantially linear targets to dolphins. However, man-made sonar could be designed to use the frequencies where nonlinear scatter can be excited from targets; for example, in the detection of sea mines in coastal waters (Leighton *et al.* 2010, 2011). Extension of the technique to radar might allow the possibility of using nonlinearities to distinguish between electronics and soil, e.g. for the detection of improvised explosive devices and covert electronics (Leighton *et al.* 2010). Lidar scatters nonlinearly from combustion products, and so a similar processing scheme could be investigated to enhance such detectors. Although TWIPS and BiaPSS could both address these applications by exploiting a similar nonlinearity, the variation in amplitude used in BiaPSS is generally simpler for electronic amplifiers and transducers to generate, than the high-fidelity pulse inversion required for TWIPS.

This work received sponsorship of G.H.C.'s studentship by DSO National Laboratories, Singapore. We are very grateful to Alastair Fothergill and the BBC Natural History Unit, and all involved in the making of *The Blue Planet*. The data reported in the paper will be publicly available from http://resource.isvr.soton.ac.uk/FDAG/TWIPS/indexold4.htm.

References

Au, W. W. L. 1993 *The sonar of dolphins*. New York, NY: Springer.

Au, W. W. L. 2004 The dolphin sonar: excellent capabilities in spite of some mediocre properties. In *High-frequency ocean acoustics* (eds M. B. Porter, M. Siderius & W. Kuperman), pp. 247–259. Melville, NY: American Institute of Physics. (doi:10.1063/1.1843019)

Au, W. W. L. & Martin, S. W. 2012 Why dolphin biosonar performs so well in-spite of mediocre 'equipment'. *IET Radar Sonar Navig.* **6**, 566–575. (doi:10.1049/iet-rsn.2011.0194)

Au, W. W. L. & Nachtigall, P. E. 1997 Acoustics of echolocating dolphins and small whales. *Mar. Freshw. Behav. Physiol.* **29**, 127–162. (doi:10.1080/10236249709379004)

Au, W. W. L., Benoit-Bird, K. J. & Kastelein, R. A. 2007 Modelling the detection range of fish by echolocating bottlenose dolphins and harbour porpoises. *J. Acoust. Soc. Am.* **121**, 3954–3962. (doi:10.1121/1.2734487)

Burdic, W. S. 1984 *Underwater acoustic system analysis*. Prentice-Hall Signal Processing series. Englewood Cliffs, NJ: Prentice-Hall, Inc.

Capus, C., Pailhas, Y., Brown, K. & Lane, D. M. 2007 Bio-inspired wideband sonar signals based on observations of the bottlenose dolphin (*Tursiops truncatus*). *J. Acoust. Soc. Am.* **121**, 594–604. (doi:10.1121/1.2382344)

Chua, G. H., White, P. R. & Leighton, T. G. 2012 Use of clicks resembling those of the Atlantic bottlenose dolphin (*Tursiops truncatus*) to improve target discrimination in bubbly water with biased pulse summation sonar. *IET Radar Sonar Navig.* **6**, 510–515. (doi:10.1049/iet-rsn.2011.0199)

Clarke, J. W. L. & Leighton, T. G. 2000 A method for estimating time-dependent acoustic cross-sections of bubbles and bubble clouds prior to the steady state. *J. Acoust. Soc. Am.* **107**, 1922–1929. (doi:10.1121/1.428474)

Clift, R., Grace, J. R. & Weber, M. E. 1978 *Bubbles, drops and particles*. San Diego, CA: Academic Press.

Commander, K. W. & Prosperetti, A. 1989 Linear pressure waves in bubbly liquid: comparison between theory and experiments. *J. Acoust. Soc. Am.* **85**, 732–746. (doi:10.1121/1.397599)

Doust, P. E. & Dix, J. F. 2001 The impact of improved transducer matching and equalisation technique on the accuracy and validity of underwater acoustic measurements. In *'Acoustical Oceanography', Proc. Institute of Acoustics, Southampton Oceanography Centre, Southampton,*

UK, 9–12 April 2001, vol. 23, Part 2 (eds T. G. Leighton, G. J. Heald, H. Griffiths & G. Griffiths), pp. 100–109. Bath, UK: Bath University Press.

Finfer, D. C., White, P. R., Chua, G. H. & Leighton, T. G. 2012 Review of the occurrence of multiple pulse echolocation clicks in recordings from small odontocetes. *IET Radar Sonar Navig.* **6**, 545–555. (doi:10.1049/iet-rsn.2011.0348)

Francois, R. E. & Garrison, G. R. 1982*a* Sound absorption based on ocean measurements. Part I. Pure water and magnesium sulfate contributions. *J. Acoust. Soc. Am.* **72**, 896–907. (doi:10.1121/1.388170)

Francois, R. E. & Garrison, G. R. 1982*b* Sound absorption based on ocean measurements. Part II. Boric acid contribution and equation for total absorption. *J. Acoust. Soc. Am.* **72**, 1879–1890. (doi:10.1121/1.388673)

Herzing, D. L. & dos Santos, M. E. 2004 Functional aspects of echolocation in dolphins. In *Advances in the study of echolocation in bats and dolphins* (eds J. A. Thomas, C. F. Moss & M. Vater), pp. 386–393. Berlin, Germany: Springer.

Houser, D. S., Martin, S. W., Bauer, E. J., Phillips, M., Herrin, T., Cross, M., Vidal, A. & Moore, P. W. 2005 Echolocation characteristics of free-swimming bottlenose dolphins during object detection and identification. *J. Acoust. Soc. Am.* **117**, 2308–2317. (doi:10.1121/1.1867912)

Leighton, T. G. 2004 From seas to surgeries, from babbling brooks to baby scans: the acoustics of gas bubbles in liquids. *Int. J. Mod. Phys. B* **18**, 3267–314. (doi:10.1142/S0217979204026494)

Leighton, T. G., Meers, S. D. & White, P. R. 2004 Propagation through nonlinear time-dependent bubble clouds and the estimation of bubble populations from measured acoustic characteristics. *Proc. R. Soc. Lond. A* **460**, 2521–2550. (doi:10.1098/rspa.2004.1298)

Leighton, T. G., Finfer, D. C., White, P. R., Chua, G. H. & Dix, J. K. 2010 Clutter suppression and classification using twin inverted pulse sonar (TWIPS). *Proc. R. Soc. A* **466**, 3453–3478. (doi:10.1098/rspa.2010.0154)

Leighton, T. G., Finfer, D. C., Chua, G. H., White, P. R. & Dix, J. K. 2011 Clutter suppression and classification using twin inverted pulse sonar in ship wakes. *J. Acoust. Soc. Am.* **130**, 3431–3437. (doi:10.1121/1.3626131)